Molecular Biology of the Cell
Vol. 11, 3617–3627, October 2000

Conditional Expression of a Truncated Fragment of Nonmuscle Myosin II-A Alters Cell Shape but Not Cytokinesis in HeLa Cells

Qize Wei and Robert S. Adelstein*

Laboratory of Molecular Cardiology, National Heart, Lung, and Blood Institute, National Institutes of Health, Bethesda, Maryland 20892

Submitted March 15, 2000; Revised July 14, 2000; Accepted August 2, 2000
Monitoring Editor: Thomas D. Pollard

A truncated fragment of the nonmuscle myosin II-A heavy chain (NMHC II-A) lacking amino acids 1–591, ΔN592, was used to examine the cellular functions of this protein. Green fluorescent protein (GFP) was fused to the amino terminus of full-length human NMHC II-A, NMHC II-B, and ΔN592 and the fusion proteins were stably expressed in HeLa cells by using a conditional expression system requiring absence of doxycycline. The HeLa cell line studied normally expressed only NMHC II-A and not NMHC II-B protein. Confocal microscopy indicated that the GFP fusion proteins of full-length NMHC II-A, II-B, and ΔN592 were localized to stress fibers. However, in vitro assays showed that baculovirus-expressed ΔN592 did not bind to actin, suggesting that ΔN592 was localized to actin stress fibers through incorporation into endogenous myosin filaments. There was no evidence for the formation of heterodimers between the full-length endogenous nonmuscle myosin and truncated nonmuscle MHCs. Expression of ΔN592, but not full-length NMHC II-A or NMHC II-B, induced cell rounding with rearrangement of actin filaments and disappearance of focal adhesions. These cells returned to their normal morphology when expression of ΔN592 was repressed by addition of doxycycline. We also show that GFP-tagged full-length NMHC II-A or II-B, but not ΔN592, were localized to the cytokinetic ring during mitosis, indicating that, in vertebrates, the amino-terminus part of mammalian nonmuscle myosin II may be necessary for localization to the cytokinetic ring.

INTRODUCTION

In eukaryotic cells, the cytoskeletal tension generated by the dynamic interaction of actin and myosin has been implicated in the regulation of cell spreading (Sanders *et al.*, 1999; van Leeuwen *et al.*, 1999), cell motility (Lauffenburger and Horwitz, 1996), cell morphology (Paterson *et al.*, 1990), and cytokinesis (De Lozanne and Spudich, 1987; Satterwhite and Pollard, 1992; Fishkind and Wang, 1995). There are at least three types of actin cytoskeleton: the cortical actin network, actin stress fibers, and actin that is involved in cell surface protrusions, including membrane ruffles and microspikes. Stress fibers are actin filament bundles emanating from the plasma membrane at focal adhesions, where clusters of integrin receptors bind to extracellular matrix proteins such as fibronectin and collagen. The assembly of myosin molecules into bipolar filaments has been shown to be necessary for the formation of actin stress fibers that are associated with focal adhesions (Verkhovsky *et al.*, 1995, 1997; Burridge and Chrzanowska-Wodnicka, 1996).

* Corresponding author: E-mail address: AdelsteR@nhlbi.nih.gov.

Conventional myosin in nonmuscle cells, also referred to as nonmuscle myosin II, is present as at least two different isoforms, II-A and II-B (Katsuragawa *et al.*, 1989; Kawamoto and Adelstein, 1991). Both isoforms are heterohexamers composed of a pair of heavy chains and two pairs of light chains. Each myosin heavy chain (MHC) contains two characteristic regions: a globular region at the amino terminus that catalyzes ATP hydrolysis and binds to actin to generate force and movement, and an α-helical carboxy-terminal tail region responsible for the formation of an extended parallel coiled-coil and the assembly of bipolar myosin filaments. The two pairs of light chains are situated at the neck junction between the motor and tail domain and are thought to be involved in regulating myosin–actin interactions and ATPase activity (for review, see Sellers, 1999).

Previous studies revealed that the two isoforms of nonmuscle myosin, II-A and II-B, showed differences in their biological properties and intracellular localization, indicating that each isoform might perform different cellular functions (Maupin *et al.*, 1994; Kelley *et al.*, 1996; Kolega, 1998). Recently, mice lacking nonmuscle myosin II-B were generated and found to develop defects in both the heart and

brain during embryonic development, suggesting an important role for NMHC II-B in these two organs (Tullio *et al.*, 1997). However, less is known about the specific functional roles of nonmuscle myosin II at a cellular level.

To understand the function of nonmuscle myosin II in cultured mammalian cells, we made use of the HeLa Tet-Off system (Clontech, Palo Alto, CA). This allowed us to regulate the expression of the protein in a reversible manner. Of note is that the HeLa cell line used in these experiments expressed only NMHC II-A (in contrast to both NMHC II-A and NMHC II-B), which simplified the system under study. We selected three different amino-terminal green fluorescent protein (GFP)-fused constructs for stable expression: full-length NMHC II-A, full-length NMHC II-B, and a truncated version of NMHC II-A lacking amino acids 1–591. The purpose of this last construct was to delete the motor domain but still retain the ability of the construct to be incorporated into the endogenous myosin filaments. Here we report that the truncated NMHC acts as a dominant-negative fragment, interfering with the myosin filaments and disrupting focal adhesions that result in alterations in HeLa cell morphology. Despite disruption of the cell morphology, these HeLa cells were able to undergo mitosis because, in contrast to the endogenous myosin, the truncated NMHC did not localize to the cleavage furrow during cytokinesis.

MATERIALS AND METHODS

Plasmid Construction

The cytomegalovirus promoter in pEGFP-C_3 (Clontech) was replaced by a tetracycline-responsive promoter that was amplified from pTRE (Clontech) by using polymerase chain reaction (PCR). The resulting plasmid vector was designated as pTRE-GFP. A DNA fragment encoding amino acids 1–1337 from NMHC II-A (Toothaker *et al.*, 1991) was amplified and subcloned into the multiple cloning site (*Hin*dIII/*Eco*RI) of pTRE-GFP to generate pTRE-GFP-HA5′. A second DNA fragment encoding amino acids 1338–1961 of NMHC II-A was amplified from pNMHCM2 described in Saez *et al.* (1990) and subcloned into an *Eco*RI/blunted-*Bam*HI site in pTRE-GFP-HA5′, generating pTRE-GFP-NMHC II-A. To generate pTRE-GFP-ΔN592, pTRE-GFP-NMHC II-A was digested with *Bam*HI and the purified larger fragment was rendered blunt and self-ligated. To generate pTRE-GFP-ΔC170 encoding amino acids 1–1791, pTRE-GFP-NMHC II-A was digested with *Afl*II/*Spe*I and the purified larger fragment was rendered blunt and self-ligated. pTRE-GFP-NMHC II-B was generated by subcloning a DNA fragment containing full-length NMHC II-B (Simons *et al.*, 1991; Phillips *et al.*, 1995) into the *Eco*RI/*Sac*II site of pTRE-GFP. For convenience, pTRE-GFP-NMHC II-A, pTRE-GFP-ΔN592, pTRE-GFP-ΔC170, and pTRE-GFP-NMHC II-B will be referred to as GFP-NMHC II-A, GFP-ΔN592, GFP-ΔC170, and GFP-NMHC II-B. In addition, a DNA fragment encoding red flourescent protein (RFP) was amplified from pDsRed1-N1 (Clontech) by using PCR and subcloned into the *Eco*47III/*Xho*I site in pEGFP-C3 to replace the EGFP, resulting pRFP-C3. A DNA fragment encoding amino acids 1–1961 of NMHC II-A was cloned into the *Hin*dIII/*Sma*I site in pRFP-C3 to generate pRFP-NMHC II-A (NMHC II-A was under the control of the cytomegalovirus promoter). All constructs were confirmed by sequencing.

Cell Culture and Transfection

HeLa Tet-Off cells (Clontech) were grown in DMEM supplemented with 10% fetal bovine serum (Life Technologies, Rockville, MD). GFP-NMHC II-A, GFP-ΔN592, or GFP-NMHC II-B was cotransfected with plasmid pTK-Hyg (Clontech), which contained the hygromycin-resistant gene. Transfection was carried out by using Lipofectamine (Life Technologies) according to the manufacturer's instructions. Colonies resistant to both 400 μg/ml G418 (Life Technologies) and 200 μg/ml hygromycin (Life Technologies) were isolated. The resulting colonies were maintained in 100 μg/ml G418, 100 μg/ml hygromycin, and 1 μg/ml doxycycline (Sigma, St. Louis, MO). Expression of the transfected genes was induced by removing doxycycline and was suppressed by adding it back to the culture.

For transient transfection, the various GFP-fusion proteins (NMHC II-A, II-B, ΔC170, or ΔN592) were cotransfected with L63RhoA (provided by Dr. Alan Hall, University College London) into HeLa Tet-Off cells by using Lipofectamine (Life Technologies). Twenty-four hours after transfection, the transfected cells were processed for immunofluorescence studies as described below.

Immunofluorescence Studies

Both NMHC II-A and II-B and ΔN592 stable cell lines were cultured in the absence of doxycycline to induce the expression of NMHC II and ΔN592. After the expression was confirmed by fluorescence microscopy and Western blot, the cells were trypsinized and grown on coverslips, fixed with 3.7% paraformaldehyde, and permeabilized with 0.5% Triton X-100. Monoclonal antibodies against human vinculin (1:500; Sigma), β-tubulin (1:1000; Sigma), Myc (1:1000; Santa Cruz Biotechnology, Santa Cruz, CA), and affinity-purified polyclonal rabbit antibodies against amino acid sequences near the carboxy terminus of NMHC II-A and NMHC II-B (anti-C, 1:1000; Phillips *et al.*, 1995) or amino terminus (anti-N; 1:50) of NMHC II-A were used. The human amino acid sequence used to generate these last antibodies was as follows: QAADKYLYVDKNFIN (Simons *et al.*, 1991). These antibodies were shown to only detect NMHC II-A and not NMHC II-B by using extracts of RBL-2H3 cells (II-A only) and COS-7 cells (II-B only). Incubation with the first antibody was carried out at a temperature of 23°C for 2 h or at 4°C overnight. The secondary antibody was rhodamine-labeled goat anti-mouse IgG or Texas Red-labeled goat anti-rabbit IgG or Alexa350 goat anti-mouse IgG (Molecular Probes, Eugene, OR). F-actin was visualized by rhodamine-phalloidin (Molecular Probes). Incubation with the secondary antibody or phalloidin was carried out at 23°C for 45 min. The coverslips were mounted with ProLong antifade kit (Molecular Probes). The images were collected by a Zeiss LSM 510 confocal microscope (Carl Zeiss, Thornwood, NY).

Immunoblot Analysis

Total cell protein from different stable cell lines was separated by SDS-6% PAGE, transferred to an Immobilon-P transfer membrane (Millipore, Bedford, MA), blocked in 5% nonfat milk, and incubated with anti-rabbit polyclonal antibodies to the carboxy terminus (anti-C; 1:5000) or the amino terminus (anti-N; 1:1000) of NMHC II-A or the carboxy terminus of NMHC II-B (1:100,000) at 4°C overnight. The blot was washed and then incubated with horseradish peroxidase-conjugated secondary antibodies (1:20,000; Pierce, Rockford, IL) at room temperature for 2 h. The blots were visualized by SuperSignal West Pico Luminol/Enhancer solution (Pierce).

Baculovirus Expression of GST-ΔN592 and Actin-binding Assay

A *Not*I site and a *Sma*I site were introduced into the 5′ and 3′ end of ΔN592, respectively, by PCR. The resulting PCR fragment containing ΔN592 was subcloned into the *Not*I/*Sma*I site of pAcGHLT-A baculovirus transfer vector (PharMingen, San Diego, CA) generating pAcGHLT-A-ΔN592. The construct was verified by nucleotide sequencing. pAcGHLT-A-ΔN592 was transfected into Sf9 cells (PharMingen) by Insect-Plus insect cell-specific liposome (Invitrogen, Carlsbad, CA) according to the manufacturer's instructions. The resulting ΔN592 virus was coinfected into Sf9 cells with virus

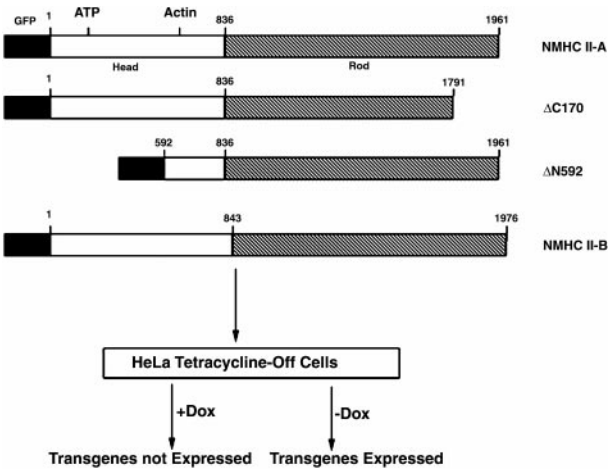

Figure 1. Schematic diagram of full-length nonmuscle myosin II-A and II-B heavy chains and the truncated NMHC II-A, ΔN592, and ΔC170 constructs. The full-length and truncated NMHC II constructs are all fused to GFP and under the control of the tetracycline-responsive promoter, so that they are only expressed in the absence of doxycycline (Dox) and expression of the transgenes will be turned off by the addition of Dox. Stable cell lines were established for each of the constructs except ΔC170. ATP- and actin-binding domains are indicated. Numbers indicate amino acid residues.

encoding both myosin light chains to increase the solubility of expressed protein (Pato *et al.*, 1996). GST-ΔN592 was purified by using glutathione beads.

For the actin-binding assay, baculovirus-expressed GST-ΔN592 protein or a cell lysate from HeLa cells containing endogenous myosin was incubated with rabbit skeletal F-actin (provided by James Sellers, National Heart, Lung, and Blood Institute) in 0.5 M NaCl, 1 mM $MgCl_2$, 40 mM 3-(*N*-morpholino)propanesulfonic acid (pH 7.0), 5 mM EGTA, 2 mM dithiothreitol, 0.1 mM phenylmethylsulfonyl fluoride, 1× protein inhibitor mix (PharMingen), on ice for 20 min, in the presence or absence of 2 mM ATP. The incubation mix was sedimented at 543,000 × *g* at 4°C for 20 min. The pellets were resuspended in the same volume of supernatant. The pellets and supernatant peptides were separated on SDS-6% PAGE, transferred to an Immobilon-P membrane and detected by using an antibody to the carboxy terminus (1:5000; anti-C) of NMHC II-A.

For analysis of possible heterodimer formation between ΔN592 and endogenous NMHC II-A, extracts of HeLa cells expressing both NMHCs were used. For actin binding in the absence of ATP, the cell lysate was first incubated with 4 units of hexokinase (Sigma) per 200 μl of cell lysate in the presence of 1 mM glucose for 30 min at 22°C before the addition of F-actin. Sedimentation and detection of myosin isoforms was as described above.

RESULTS

Inducible Expression of Full-length Myosin II-A, II-B, and ΔN592-GFP Fusion Proteins

Three different amino-terminal GFP fusion polypeptides were expressed in stably transfected HeLa Tet-Off cell lines. As diagramed in Figure 1, one GFP fused polypeptide consisted of the full-length human NMHC II-A, the second of NMHC II-B, and the third of a GFP-fused truncated form of the NMHC II-A starting at amino acid 592 and continuing to the carboxy-terminal end, amino acid 1961 (ΔN592). Each of the three polypeptides was expressed only when doxycycline was removed from the HeLa cell culture. These three constructs and a fourth plasmid expressing a GFP-fused polypeptide containing amino acids 1–1791 of NMHC II-A (ΔC170, Figure 1) were also used for transient cotransfection with the RhoA dominant active mutant L63RhoA as described below.

Figure 2A is an immunoblot by using primary antibodies to NMHC II-A raised to the carboxy-terminal (lanes 1–4) and to the amino-terminal (lanes 5 and 6) amino acid sequence of the NMHC. The immunoblot shows that, in the presence of doxycycline, no full-length GFP-NMHC II-A (lane 1) and no GFP-ΔN592 fragment (lane 3) is expressed, whereas in the absence of doxycycline, both GFP-NMHC II-A and the GFP-ΔN592 fragments are expressed at comparable amounts to the endogenous NMHC II-A (lanes 2 and 4). The figure also shows that antibodies generated to the amino-terminal sequence of human NMHC II-A only recognize the full-length MHC and not the ΔN592 fragment, which is expressed in the absence of doxycycline (Figure 2A, lanes 5 and 6). This antibody, in contrast to the carboxy-terminal antibody, can therefore be used to distinguish the full-length NMHC from ΔN592. Lanes 7 and 8 are extracts of HeLa cells stably transfected with GFP-NMHC II-B and immunoblotted with antibodies raised against the carboxy-terminal amino acid sequence of NMHC II-B. Lane 7 confirms that this HeLa cell line does not express NMHC II-B, but only NMHC II-A (lane 1). Lane 8 shows that, following withdrawal of doxycycline, these transfected cells express GFP-NMHC II-B.

To characterize the ΔN592 fragment, we used baculovirus-expressed ΔN592-GST fusion protein in an actin-binding assay. Figure 2B shows that, unlike endogenous myosin II-A, which binds to actin in the absence, but not the presence of ATP (lanes 5–8), the ΔN592 fragment was incapable of binding to actin in the presence or absence of ATP (lanes 1–4). To address the question of whether ΔN592 could form a heterodimer with the endogenous NMHC II-A, the cell extracts from HeLa cells expressing ΔN592 were analyzed by using an actin-binding assay. As shown in Figure 2C, in the absence of ATP, endogenous full-length NMHC II-A from these cells bound to actin and sedimented in the pellet (lanes 1). In contrast, very little ΔN592 was sedimented with NMHC II-A and no full-length NMHC II-A remained in the supernatant (lane 2). In the presence of ATP, both endogenous NMHC II-A and ΔN592 failed to bind to actin and remained in the supernatant (lanes 3 and 4). These results confirmed that ΔN592 lost its ability to bind to actin. More importantly, they showed that no significant amount of ΔN592 and NMHC II-A formed heterodimers.

Dominant-Negative Effects of Expressed ΔN592

Expression of the GFP-ΔN592 fragment resulted in the cells rounding up (compare Figure 3, g and h), whereas expression of GFP-NMHC II-A had no discernible effect on HeLa cell morphology (compare Figure 3, c and d). Note that, in the presence of doxycycline, neither ΔN592 nor full-length NMHC II-A are expressed (Figure 3, b and f) and, as expected, there is no change in HeLa cell morphology (Figure 3, d and h). Approximately 70% of the cells transfected with GFP-ΔN592 rounded up over a period of 3 to 5 days in the absence of doxycycline. This was the case for all three stable

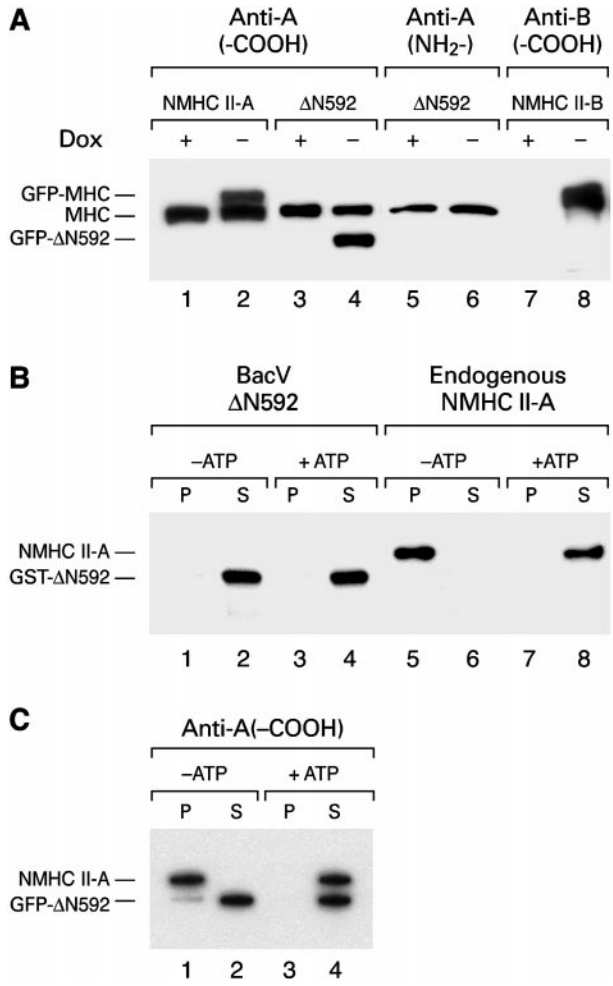

Figure 2. Immunoblot analysis and actin-binding studies of NMHC-II and ΔN592. (A) Inducible expression of GFP-NMHC II-A, II-B, and GFP-ΔN592 in HeLa Tet-Off cells. The stable cell lines cultured with (+) or without (−) doxycycline (Dox) for 3 d were subjected to immunoblot analysis by using antibodies raised against amino acids at the carboxy terminus (anti-A, -COOH, lanes 1–4) or at the amino terminus (anti-A, NH_2-, lanes 5 and 6) of the myosin II-A heavy chain as well as antibodies raised against the carboxy terminus (anti-B, -COOH, lanes 7 and 8) of the myosin II-B heavy chain. The HeLa Tet-Off cell line from Clontech does not contain endogenous NMHC II-B (lane 7), but introduction of a plasmid encoding NMHC-B into these cells by stable transfection resulted in NMHC II-B expression in the absence (lane 8), but not in the presence of Dox (lane 7). (B) Immunoblot demonstrating that ΔN592 does not bind to actin. Purified baculovirus-expressed ΔN592 does not cosediment with actin in the presence or in the absence of ATP (lanes 1 and 3). In contrast, endogenous NMHC II-A binds to actin in the absence of ATP (lane 5), but not in the presence of ATP (lane 8). P, pellet; S, supernatant. (C) GFP-ΔN592 does not dimerize with endogenous NMHC II-A. Cell extracts from HeLa cells expressing GFP-ΔN592 and endogenous NMHC II-A were incubated with F-actin in the absence (lanes 1 and 2) or presence (lanes 3 and 4) of Mg^{2+}-ATP, followed by sedimentation resulting in pellet (p) and supernatant (s) fractions. GFP-ΔN592 does not bind to actin in the absence or presence of ATP (lanes 2 and 4). Endogenous NMHC II-A bound to actin in the absence of ATP (lane 1). Note that only a very small amount of GFP-ΔN592 cosedimented with endogenous NMHC II-A (lane 1). This was most likely due to minor trapping of ΔN592 in the actin pellet.

cell lines generated with this construct. As another control, we introduced the full-length construct of GFP-NMHC II-B into this HeLa cell line. Expression of this construct did not cause the cells to alter their morphology (Figure 4Aa). In the cell shown in Figure 4Ac, NMHC II-A (red) was the predominant isoform present in the apices and NMHC II-B (green) was more abundant in the cytoplasm. Both isoforms colocalized in the cortex (yellow). The presence of NMHC II-A in the apices is in contrast to the localization reported by Maupin *et al.* (1994) for a HeLa cell line that, unlike the one used in these experiments, constitutively expresses both isoforms of myosin. However, the localization pattern seen in Figure 4Ac was not consistently observed in all transfected cells.

Stress fibers were not easily visualized in this particular HeLa cell line, even after stimulation by serum or lysophosphatidic acid. We, therefore, transfected these cells with a dominant active mutant of RhoA (L63RhoA), which has been reported to induce stress fiber formation and bundling of actin filaments (Hall, 1998). As shown in Figure 4B, transiently transfected GFP-NMHC II-A (a), GFP-ΔN592 (b), and GFP-NMHC II-B (d) all form stress fibers. In contrast, GFP-ΔC170, which lacks the assembly competent domain in the myosin rod (Sohn *et al.*, 1997; Figure 4Bc), does not form stress fibers.

Expression of ΔN592 Causes Reversible Disruption of Myosin Filaments

Because ΔN592 contains the entire rod and tail region of NMHC II-A, we expected that it would be incorporated into the endogenous myosin filaments, but that it might interfere with myosin function because it lacks the ATP-binding region and cannot interact with actin (Figure 2B).

Figure 5A details the change in HeLa cell morphology following the expression of GFP-ΔN592. The left images are confocal images of GFP-ΔN592 transfected cells and the middle images are rhodamine images of endogenous NMHC II-A detected with an antibody raised to the NH_2-terminal sequence. These antibodies distinguish between ΔN592 and the endogenous myosin because the former, truncated peptide, lacks amino acids 1–591. The images on the right merge the two images.

In the presence of doxycycline (i.e., when ΔN592 is not expressed), ΔN592 transfected HeLa cells have organized myosin filaments and maintain a typical flattened morphology (endogenous myosin detected with a rhodamine-conjugated 2° antibody) (Figure 5A, b and c). After being replated for 1 d in the absence of doxycycline, the ΔN592 fragment can be detected by itself (green) as well as colocalizing with the endogenous myosin filaments (orange and yellow areas, Figure 5Af). By day 2, the cells begin to lose their organized myosin filaments and take on a more rounded shape, which is easily seen by day 4. Note that the colocalization of the ΔN592 with endogenous NMHC II-A continues in the rounded cells (yellow color, Figure 5A, i and l).

In contrast to the 4 days that were required for the development of the phenotype following expression of ΔN592, GFP-ΔN592 expression was completely repressed and the flattened morphology of the HeLa cells was restored within 16 h after addition of doxycycline to the culture (Figure 5Ao).

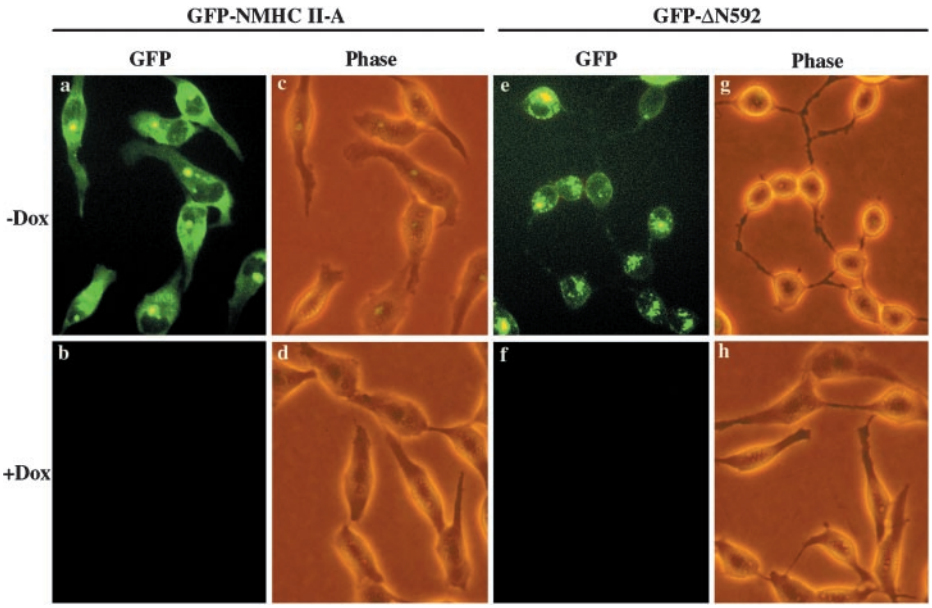

Figure 3. Cell rounding induced by the expression of GFP-ΔN592, but not the full-length myosin heavy chain (NMHC II-A) in HeLa Tet-Off cells. Cells were cultured for 3 d without Dox (a, c, e, and g) or with Dox (b, d, f, and h). The images were taken from live cells by using an Axivert 35 microscope (Carl Zeiss). Note the presence of the GFP signal only in a and e (−Dox) and the rounded morphology of cells expressing GFP-ΔN592 (e and g) in contrast to cells expressing GFP-NMHC II-A (a and c). The original magnification was 320×.

Figure 5B demonstrates evidence for incorporation of ΔN592 into myosin II-A filaments in cells transiently transfected with L63RhoA, GFP-ΔN592, and RFP-NMHC II-A. The yellow filaments contain both the truncated and full-length myosin. We made use of the RFP-NMHC II-A construct because the antibody to the NH_2-terminal end of endogenous myosin II-A did not detect the bundled filaments following transfection with L63RhoA.

Rearrangement of Actin Filaments Induced by Expression of ΔN592

Because actin filaments play a major role in defining cell polarity and morphology, we used rhodamine-labeled phalloidin to visualize actin in cells expressing full-length GFP-NMHC II-A and the GFP-ΔN592 construct. Figure 6A, a–c, are confocal images of GFP-NMHC II-A, phalloidin-labeled actin, and a merged image, respectively, in cells in the absence of doxycycline. Both actin (red) and myosin (green) fibers can be visualized and, in some areas, they colocalize (yellow, orange). Introduction of the GFP-ΔN592 construct, in the presence of doxycycline, had no effect on the actin filaments (Figure 6A, e and f), whereas expression of the ΔN592 fragment showed that, in some areas, similar to the full-length NMHC, it colocalized with actin filaments (yellow, orange) and some areas it could be detected alone (Figure 6Ai). When cells were cultured in the absence of doxycycline for 4 d, they began to round up and the actin filaments were rearranged (Figure 6A, k and l).

Figure 6B shows three different focal planes of a representative field with two rounded cells (indicated by arrows) and one flattened cell (indicated by an arrowhead). The two rounded cells expressing GFP-ΔN592 show rearrangement of actin filaments, whereas the flattened cell (not expressing ΔN592) shows organized actin filaments (Figure 6B, c, f, and i).

Disruption of Focal Adhesion Complexes by Expression of GFP-ΔN592

We also examined the HeLa cells to see whether disruption of the actin-myosin filament network induced by the expression of GFP-ΔN592 had any effect on focal adhesion complexes because actin stress fibers are known to be associated with these complexes. ΔN592 transfected cell lines were cultured on coverslips for 4 d in the presence (Figure 7, a and c) or in the absence (Figure 7, b and d) of doxycycline and focal adhesions were detected by using an anti-vinculin antibody (Figure 7, c and d). Whereas cells transfected with GFP-ΔN592 showed numerous focal adhesion complexes in the presence of doxycycline when GFP-ΔN592 is not expressed (Figure 7, a and c), these complexes disappeared and vinculin showed a diffuse staining pattern following expression of ΔN592 (Figure 7, b and d).

ΔN592 Does Not Interfere with Cytokinesis

We noted that HeLa cells transfected with GFP-ΔN592 were capable of undergoing mitosis, even in the absence of doxycycline. This suggested that ΔN592 might not localize to the cleavage furrow during cytokinesis. Therefore, we studied the localization of three different NMHC constructs, GFP-NMHC II-A, GFP-ΔN592, and GFP-NMHC II-B, in stably transfected HeLa cells during cytokinesis, while visualizing tubulin with a rhodamine-labeled antibody (red). Figure 8, c and d, show that GFP-NMHC II-A introduced into these HeLa cells can localize to the contractile ring during telophase. In contrast, GFP-ΔN592, which shows a similar distribution to full-length myosin II-A during prophase and metaphase, although forming somewhat larger aggregates, did not localize to the cytokinetic ring during telophase (Figure 8, g and h). This suggested that either all or part of the missing fragment (a.a. 1–591) might be required for localization of the MHC. As a control, we expressed full-length NMHC II-B, which is not present in this cell line

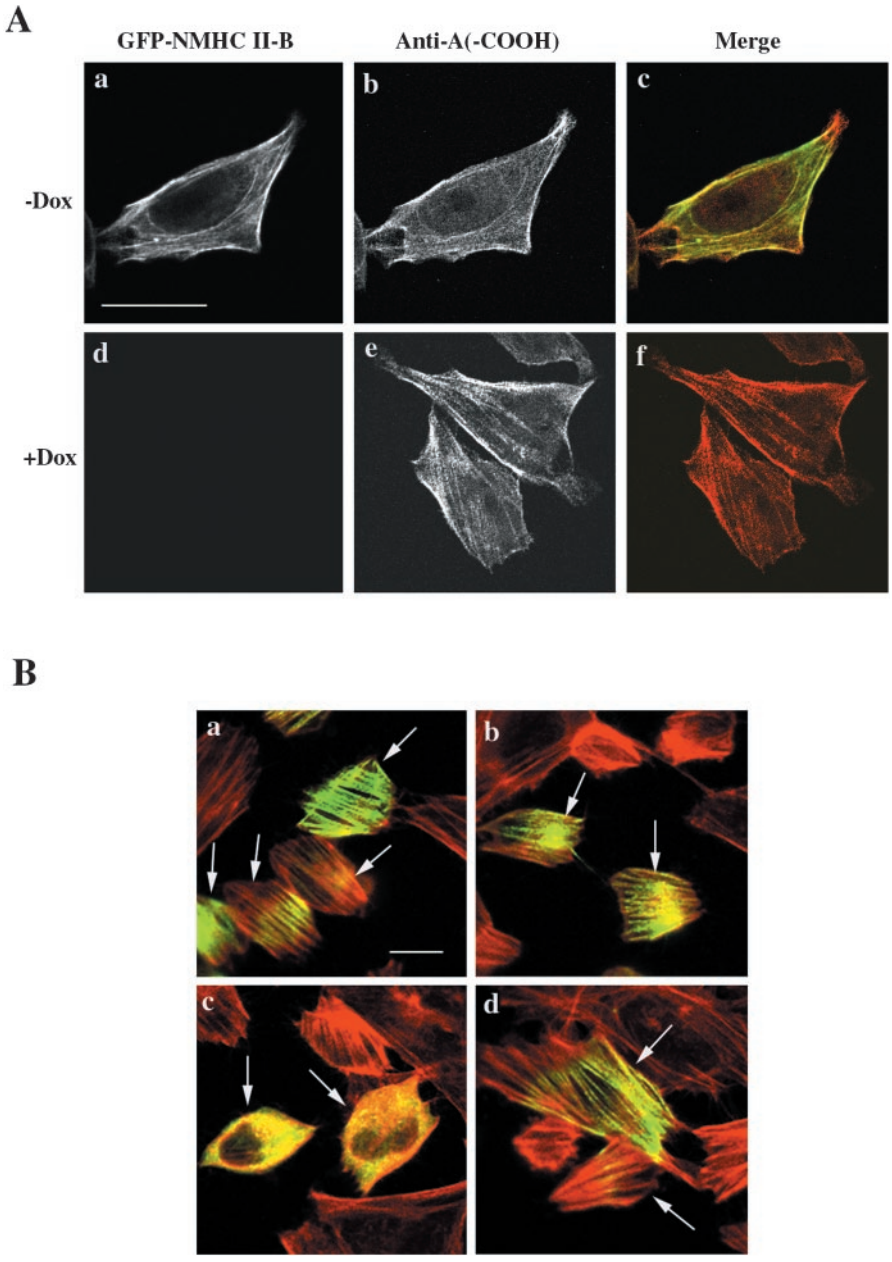

Figure 4. Colocalization of myosin II-B GFP-fusion protein and endogenous myosin II-A in HeLa Tet-Off cells and formation of myosin filaments following transfection of L63RhoA. (A) Full-length NMHC II-B was visualized by using GFP in the absence of doxycycline (a) and endogenous NMHC II-A was visualized by using antibodies to the carboxy-terminal sequence (b, e, and f). The distribution of both isoforms (II-B, green; II-A, red; colocalization, yellow) is shown in c; d, e, and f are from an experiment carried out in the presence of Dox. (B) Myosin filament formation induced by the transient expression of dominant active RhoA mutant L63RhoA. HeLa Tet-Off cells were transiently transfected with L63RhoA, along with NMHC II-A (a), ΔN592 (b), ΔC170 (c), or NMHC II-B (d), respectively. Transfected cells were visualized by GFP (green), phalloidin (red), and Myc antibody followed by Alexa 350 antimouse conjugate IgG (blue, to detect myc-tagged L63RhoA expression; our unpublished data). Arrows indicate the cells expressing both GFP-tagged myosin and L63RhoA. Note that NMHC II-A (a), ΔN592 (b), and NMHC II-B (d), but not ΔC170 (c) form filaments upon expression of L63RhoA. Bar, 20 μm.

(Figure 2A, lane 7), producing stably transfected cells. Similar to NMHC II-A, and in contrast to ΔN592, NMHC II-B localizes to the cleavage furrow and midbody (Figure 8, k and l).

DISCUSSION

In this article, we demonstrate that nonmuscle myosin II-A is required for the maintenance of cell morphology. The truncated myosin fragment (ΔN592) used in our study has been shown to act as a dominant-negative fragment, by being incorporated into the myosin filaments and actin stress fibers, and thereby destabilizing focal adhesions and leading to cell rounding.

Myosin II filament formation has been studied intensively revealing that the coiled-coil tail region of nonmuscle myosin is required for filament formation (Warrick and Spudich, 1987; Moores and Spudich, 1998; Murakami *et al.*, 1998). A detailed study of skeletal muscle myosin showed that a sequence of 29 amino acids near the carboxy terminus, referred to as the assembly competence domain (ACD), is critical for myosin filament assembly (Sohn *et al.*, 1997). ΔN592, which retains the ACD, is able to form filaments when transfected into HeLa cells, although some evidence for aggregation can be seen, particularly just before cytokinesis. Using antibodies specific to the amino terminus of the endogenous full-length myosin and a GFP-labeled truncated

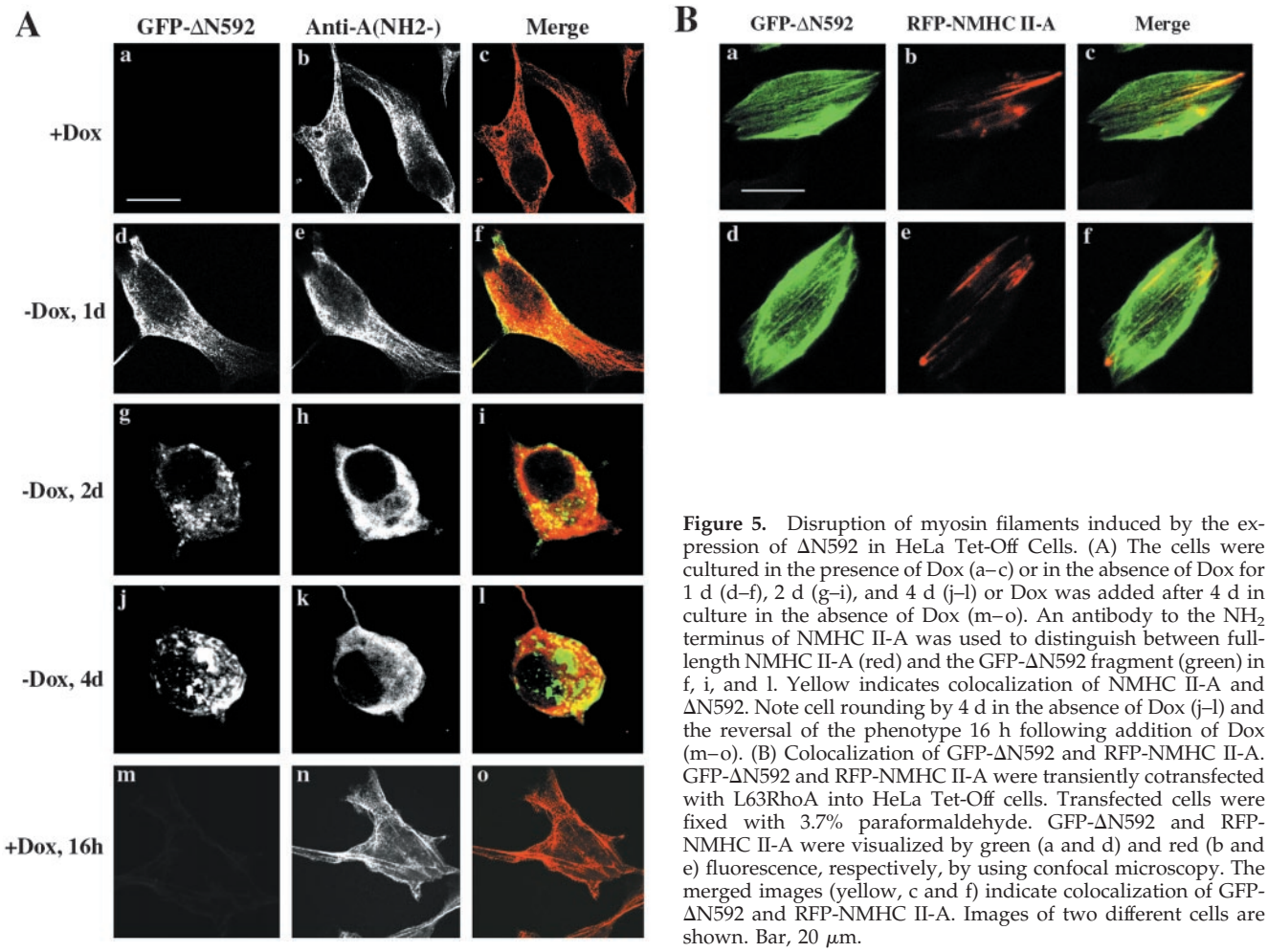

Figure 5. Disruption of myosin filaments induced by the expression of ΔN592 in HeLa Tet-Off Cells. (A) The cells were cultured in the presence of Dox (a–c) or in the absence of Dox for 1 d (d–f), 2 d (g–i), and 4 d (j–l) or Dox was added after 4 d in culture in the absence of Dox (m–o). An antibody to the NH_2 terminus of NMHC II-A was used to distinguish between full-length NMHC II-A (red) and the GFP-ΔN592 fragment (green) in f, i, and l. Yellow indicates colocalization of NMHC II-A and ΔN592. Note cell rounding by 4 d in the absence of Dox (j–l) and the reversal of the phenotype 16 h following addition of Dox (m–o). (B) Colocalization of GFP-ΔN592 and RFP-NMHC II-A. GFP-ΔN592 and RFP-NMHC II-A were transiently cotransfected with L63RhoA into HeLa Tet-Off cells. Transfected cells were fixed with 3.7% paraformaldehyde. GFP-ΔN592 and RFP-NMHC II-A were visualized by green (a and d) and red (b and e) fluorescence, respectively, by using confocal microscopy. The merged images (yellow, c and f) indicate colocalization of GFP-ΔN592 and RFP-NMHC II-A. Images of two different cells are shown. Bar, 20 μm.

construct, we found evidence for colocalization of the two isoforms as early as day 1 following replating. This colocalization persists throughout the 3 d that are required for the cells to lose their flattened morphology and round up. RhoA has been shown to induce stress fiber formation (Hall, 1998). In this work, we also demonstrate that expression of a dominant active mutant of RhoA, L63RhoA, leads to the bundling of stress fibers containing GFP-tagged NMHC II-A, II-B, and ΔN592 filaments. However, deletion of the carboxy-terminal sequence (a.a. 1792–1961) that includes the ACD from both full-length GFP-NMHC II-A (Figure 4Bc) and GFP-ΔN592 (our unpublished data) results in diffuse distribution of these GFP-fusion peptides. These results agree with a previous report that studied sarcomeric myosin assembly (Sohn *et al.*, 1997).

ΔN592 is missing the ATP-binding region, but does contain the actin-binding region (Rayment *et al.*, 1993). However, ΔN592 has lost the ability to bind to actin, confirming that the binding of myosin to actin requires a specific tertiary structure of the myosin head and that deletion of amino acids 1–591 disrupts this tertiary structure. Thus, ΔN592 retains the property of filament assembly and the ability to be incorporated into endogenous myosin, but cannot bind to actin, allowing it to act as a dominant-negative mutant in the HeLa Tet-Off cells. We found no evidence for the formation of a significant amount of heterodimers between endogenous NMHC II-A and GFP-ΔN592. Figure 2C shows that practically none of the ΔN592 construct cosedimented with full-length NMHC II-A bound to actin in the absence of ATP and only homodimers of ΔN592 remained in the supernatant. This result, together with the absence of full-length NMHC II-A in immunoprecipitates when antibodies to GFP were used to immunoprecipitate GFP-ΔN592 from HeLa cells expressing both isoforms (our unpublished data), suggested that the formation of heterodimers between ΔN592 and endogenous NMHC II-A does not play a major role in the morphological changes in these HeLa cells.

Expression of the ΔN592 construct in HeLa cells induced a marked alteration in cell morphology, resulting in a loss of focal adhesions and assumption of a round shape by >70% of the cells. It is of note that it took 3 to 5 d for the transfected cells to round up. This is not because of a delay in the induction of the expression of ΔN592 following removal of doxycycline because the cell lines were allowed to express the transgene for at least 24 h before being replated and analyzed, and the expression level of ΔN592 did not change

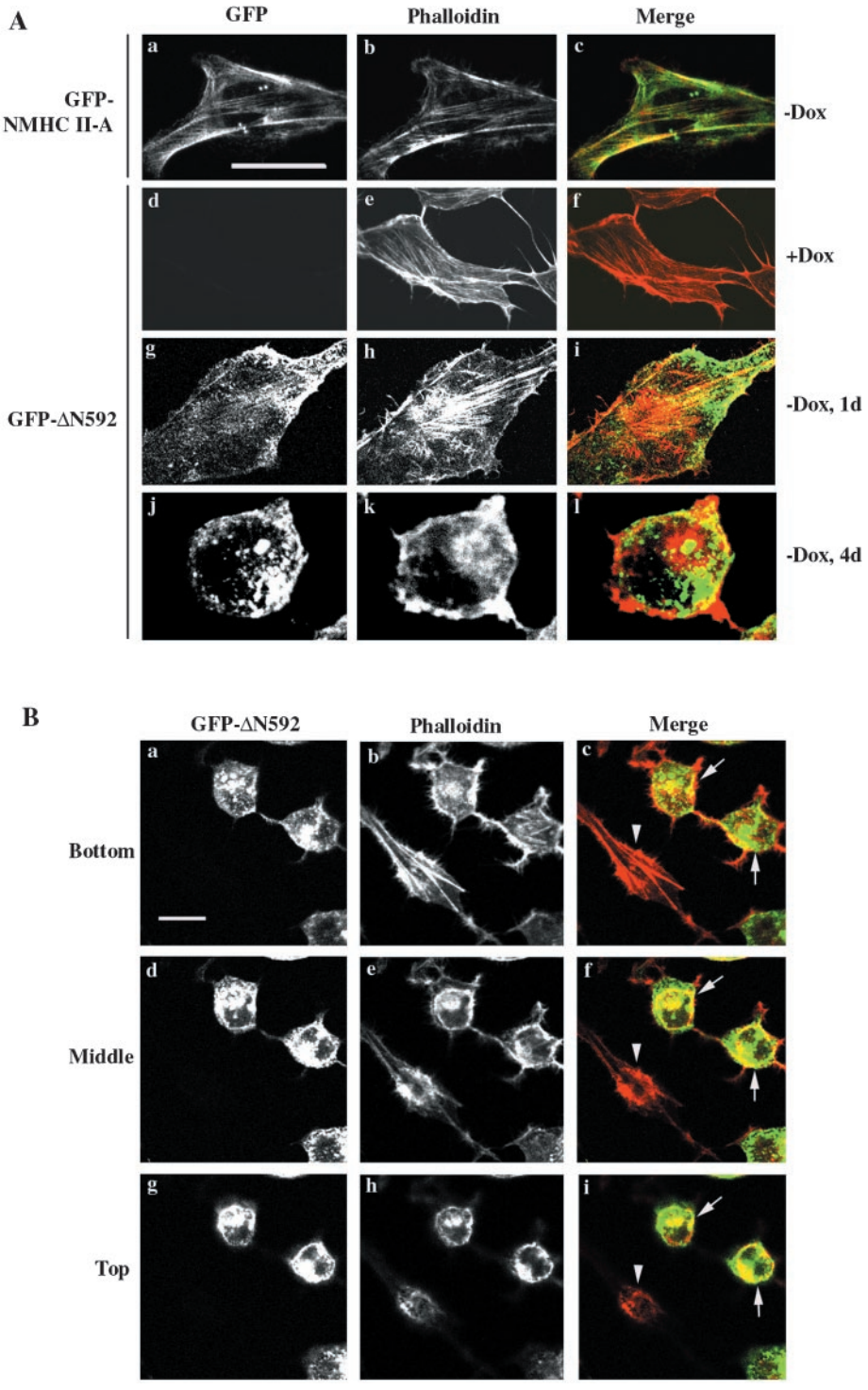

Figure 6. Rearrangement of actin filaments induced by ΔN592. (A) GFP-NMHC II-A transfected stable cell lines were cultured in the absence of Dox (a–c). Some of the full-length myosin (green) colocalizes with actin (red) to give a yellow image (c). GFP-ΔN592 stable cells were cultured in the presence of Dox (d–f) or in the absence of Dox for 1 d (g–i) or 4 d (j–l). Rearrangement of actin filaments (red) can be seen by day 4 in the absence of Dox. Green indicates ΔN592 and yellow shows areas of overlap between actin (red) and ΔN592 (green). (B) Images of a field after day 4 in the absence of Dox, with two rounded cells (arrows, expressing ΔN592) and one flat cell (arrowhead, not expressing ΔN592) were collected by Z-stack and three different focal planes (bottom, middle, and top) are shown. Bar, 20 μm .

after this time point. We also confirmed that the expression of ΔN592 did not have an effect on the expression of endogenous NMHC II-A (Figure 2A, lanes 3 and 4). Therefore, one explanation is that ΔN592 can only be incorporated very slowly into the dynamic myosin filament assembly–disassembly process described previously by Giuliano and Taylor (1990). In contrast, the rounded morphology of HeLa cells reversed to a spindle morphology within 16 h after readdition of doxycycline and organized myosin filaments reappeared, suggesting that the endogenous myosin is quickly

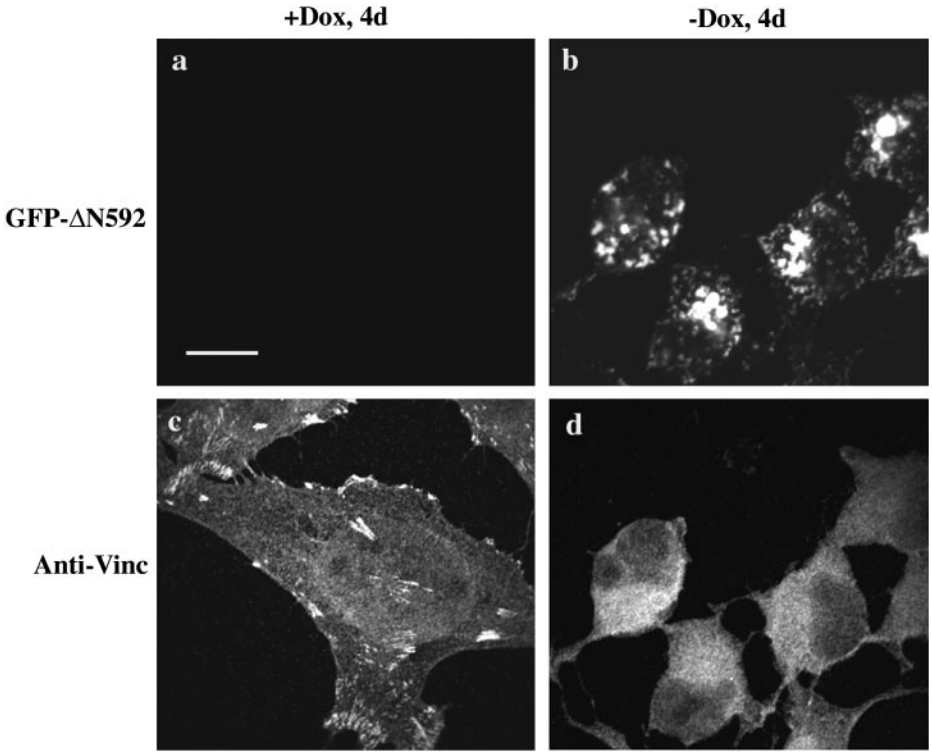

Figure 7. Disappearance of focal adhesions in GFP-ΔN592 transfected cells. (c) Presence of focal adhesions, detected with antibodies to vinculin, in the presence of Dox (GFP-ΔN592 not expressed, a). (d) Focal adhesions are disrupted following expression of GFP-ΔN592 (b) in the absence of Dox. Bar, 20 μm.

reassembled into functional bipolar filaments, which are required for the restoration of the normal flattened morphology. It is also possible that the ΔN592 fragment is degraded much more rapidly than the endogenous myosin.

A round cell morphology is associated with both normal and pathological cellular processes, such as cell transformation, mitosis, and apoptosis. For example, transformed cells are devoid of stress fibers and it has been reported that disruption of the actomyosin–cortactin complex plays a role in the ras-induced transformation of NIH3T3 cells (He *et al.*, 1998). However, at present, we have no evidence that these HeLa cells have undergone transformation following the

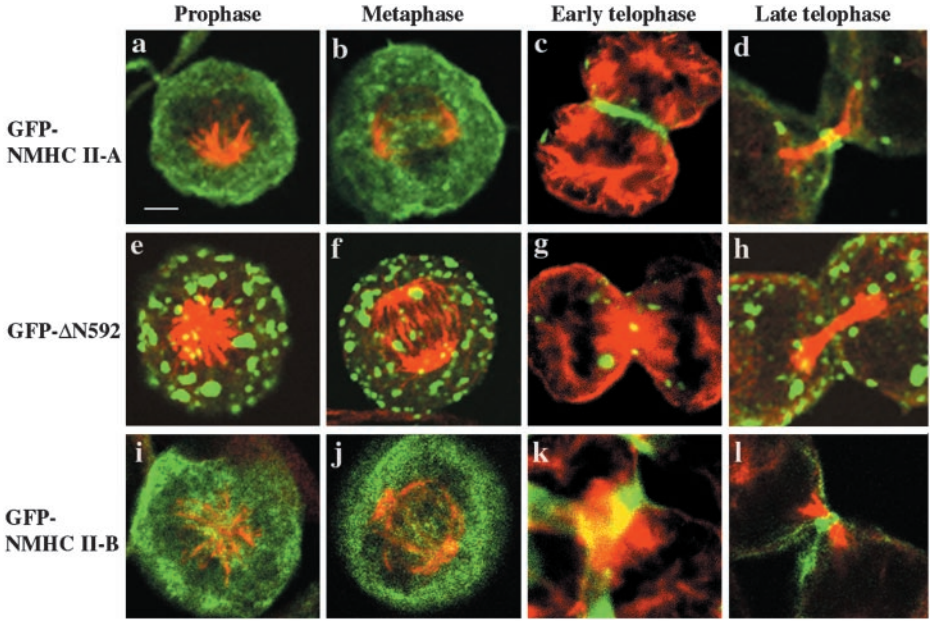

Figure 8. GFP-ΔN592 does not localize to the cytokinetic ring. GFP-NMHC II-A is distributed throughout the cytoplasm during prophase and metaphase (a and b) and localized to the cleavage furrow during early telophase (c) and the midbody during late telophase (d). ΔN592 shows a similar distribution to full-length myosin II-A during prophase and metaphase, although forming more aggregates (e–h). Note, however, that, unlike full-length NMHC II-A, it does not localize to the cleavage furrow during early telophase (g) or the midbody during late telophase (h). Transfection of HeLa cells with GFP-NMHC II-B, which is not normally expressed in these cells, shows that similar to full-length GFP-NMHC II-A, and in contrast to ΔN592, it localized to the cleavage furrow during early telophase (k) and the midbody during late telophase (i). Tubulin is detected by a rhodamine-labeled secondary antibody (red). Bar, 5 μm.

loss of NMHC II-A function. The rounded cells induced by expression of ΔN592 are not undergoing apoptosis because neither an apoptotic nucleus nor DNA fragmentation was found (our unpublished data). During mitosis, cells lose both their actomyosin stress fibers and focal adhesions. Currently, the mechanism underlying cell rounding with the onset of mitosis is unclear, but spatial rearrangement and/or disruption of actomyosin fibers is believed to play a role in this process. Several studies have suggested that inactivation of myosin Mg^{2+}-ATPase activity is correlated with the cell rounding at mitosis (Satterwhite *et al.*, 1992; Yamakita *et al.*, 1994). Furthermore, inhibition of myosin Mg^{2+}-ATPase activity by butanedione monoxime did not block cell rounding during mitosis, suggesting that myosin activity is not required (Cramer and Mitchison, 1997). When cells exit mitosis, the rounded mitotic cells begin to spread with reappearance of actomyosin stress fibers and focal adhesions. It has been shown that nonmuscle myosin is involved in postmitotic cell spreading based on butanedione monoxime inhibition experiments (Cramer and Mitchison, 1995). Their findings suggest two possibilities for the cell rounding induced by the expression of ΔN592 with respect to cell mitosis. First, the mitotic cells could not spread normally after exiting mitosis because myosin functions were interrupted by ΔN592. Second, mitotic cells are able to spread upon exiting mitosis, but round up later because of the disruption of myosin functions. We believe each of these possibilities could account for the alteration in morphology induced by the expression of ΔN592.

Maintenance and alteration of cell morphology is an important consequence of the signal transduction pathways between cells and also between the extracellular matrix and cells. For example, Swiss 3T3 cells rounded up with disruption of stress fibers following microinjection of the RhoA inhibitor c3 transferase (Paterson *et al.*, 1990). Moreover, cell rounding induced by the loss of stress fibers and focal adhesions has also been reported in Swiss 3T3 cells expressing Rnd1, a member of the Rho family (Nobes *et al.*, 1998). In most, but not all studies, the effect on the actin cytoskeleton was analyzed and emphasized. In contrast, Chrzanowska-Wodnicka and Burridge (1996) and the present study focus on the role of nonmuscle myosin II. Whereas the former study emphasizes the role of myosin phosphorylation, the present study emphasizes the importance of myosin filament formation in maintaining focal adhesion and normal cell morphology.

Despite their abnormal, rounded morphology, the cells transfected with ΔN592 were capable of undergoing cytokinesis. Although, at first, this seemed to contradict the dominant-negative effect found with respect to cell morphology and focal adhesion distribution, confocal microscopy of the mitotic cells showed that, unlike the nonmitotic cells, ΔN592 was not incorporated into the endogenous filaments of mitotic cells, nor could it localize to the cleavage furrow, as did the full-length NMHC II-A. This suggested that, unlike the findings of Spudich and colleagues for *Dictyostelium* myosin (Zang *et al.*, 1997; Zang and Spudich, 1998), mammalian myosin II requires a sequence(s) amino terminal to residue 592 to localize to the cleavage furrow. We also expressed NMHC II-B, an isoform not found in this line of HeLa cells, and found that it was capable of localizing to the cleavage furrow along with the endogenous NMHC II-A. However, further studies will be needed to determine which residues in the 591 a.a. amino-terminal fragment are required for localization of NMHC II-B.

One important function of nonmuscle myosin II filaments is to mediate the tension on actin filaments that are involved in the clustering of the integrin molecules that make up the focal adhesions. Because vinculin is a known component of these cell-matrix structures, we reasoned that disruption of the myosin filaments might result in a redistribution of vinculin. In Figure 7, we show that expression of the dominant-negative mutant ΔN592 causes a redistribution of vinculin in the HeLa cells along with a loss of focal adhesion. Taken together, these data strongly support a role for nonmuscle myosin II in normal cell morphology and in formation of focal adhesions.

ACKNOWLEDGMENTS

We thank Dr. Mary Anne Conti for characterization and purification of the amino-terminal NMHC-A antibody and for reading the manuscript, and Dr. James Sellers for constructive criticism and advice. We also thank Dr. Christian A. Combs for help and advice on the use of the confocal microscope. Catherine S. Magruder and Sophia A. Kosh are acknowledged for expert editorial assistance.

REFERENCES

Burridge, K., and Chrzanowska-Wodnicka, M. (1996). Focal adhesions, contractility, and signaling. Annu. Rev. Cell. Dev. Biol. *12*, 463–518.

Chrzanowska-Wodnicka, M., and Burridge, K. (1996). Rho-stimulated contractility drives the formation of stress fibers and focal adhesions. J. Cell Biol. *133*, 1403–1415.

Cramer, L.P., and Mitchison, T.J. (1995). Myosin is involved in postmitotic cell spreading. J. Cell Biol. *131*, 179–189.

Cramer, L.P., and Mitchison, T.J. (1997). Investigation of the mechanism of retraction of the cell margin and rearward flow of nodules during mitotic cell rounding. Mol. Biol. Cell *8*, 109–119.

De Lozanne, A., and Spudich, J.A. (1987). Disruption of the *Dictyostelium* myosin heavy chain gene by homologous recombination. Science *236*, 1086–1091.

Fishkind, D.J., and Wang, Y.L. (1995). New horizons for cytokinesis. Curr. Opin. Cell Biol. *7*, 23–31.

Giuliano, K.A., and Taylor, D.L. (1990). Formation, transport, contraction, and disassembly of stress fibers in fibroblasts. Cell. Motil. Cytoskeleton *16*, 14–21.

Hall, A. (1998). Rho GTPases and the actin cytoskeleton. Science *279*, 509–514.

He, H., Watanabe, T., Zhan, X., Huang, C., Schuuring, E., Fukami, K., Takenawa, T., Kumar, C.C., Simpson, R.J., and Maruta, H. (1998). Role of phosphatidylinositol 4,5-bisphosphate in Ras/Rac-induced disruption of the cortactin-actomyosin II complex and malignant transformation. Mol. Cell. Biol. *18*, 3829–3837.

Katsuragawa, Y., Yanagisawa, M., Inoue, A., and Masaki, T. (1989). Two distinct nonmuscle myosin-heavy-chain mRNAs are differentially expressed in various chicken tissues. Eur. J. Biochem. *184*, 611–616.

Kawamoto, S., and Adelstein, R.S. (1991). Chicken nonmuscle myosin heavy chains: differential expression of two mRNAs and evidence for two different polypeptides. J. Cell Biol. *112*, 915–924.

Kelley, C.A., Sellers, J.R., Gard, D.L., Bui, D., Adelstein, R.S., and Baines, I.C. (1996). *Xenopus* nonmuscle myosin heavy chain isoforms

have different subcellular localizations and enzymatic activities. J. Cell Biol. *134*, 675–687.

Kolega, J. (1998). Cytoplasmic dynamics of myosin IIA and IIB: spatial "sorting"of isoforms in locomoting cells J. Cell Sci. *111*, 2085–2095.

Lauffenburger, D.A., and Horwitz, A.F. (1996). Cell migration: a physically integrated molecular process. Cell *84*, 359–369.

Maupin, P., Phillips, C.L., Adelstein, R.S., and Pollard, T.D. (1994). Differential localization of myosin-II isozymes in human cultured cells and blood cells. J. Cell Sci. *107*, 3077–3090.

Moores, S.L., and Spudich, J.A. (1998). Conditional loss-of-myosin-II-function mutants reveal a position in the tail that is critical for filament nucleation. Mol. Cell *1*, 1043–1050.

Murakami, N., Chauhan, V.P., and Elzinga, M. (1998). Two nonmuscle myosin II heavy chain isoforms expressed in rabbit brains: filament forming properties, the effects of phosphorylation by protein kinase C and casein kinase II, and location of the phosphorylation sites. Biochemistry *37*, 1989–2003.

Nobes, C.D., Lauritzen, I., Mattei, M.G., Paris, S., Hall, A., and Chardin, P. (1998). A new member of the Rho family, Rnd1, promotes disassembly of actin filament structures and loss of cell adhesion. J. Cell Biol. *141*, 187–197.

Paterson, H.F., Self, A.J., Garrett, M.D., Just, I., Aktories, K., and Hall, A. (1990). Microinjection of recombinant p21rho induces rapid changes in cell morphology. J. Cell Biol. *111*, 1001–1007.

Pato, M.D., Sellers, J.R., Preston, Y.A., Harvey, E.V., and Adelstein, R.S. (1996). Baculovirus expression of chicken nonmuscle heavy meromyosin II-B. J. Biol. Chem. *271*, 2689–2695.

Phillips, C.L., Yamakawa, K., and Adelstein, R.S. (1995). Cloning of the cDNA encoding human nonmuscle myosin heavy chain-B and analysis of human tissues with isoform-specific antibodies. J. Muscle Res. Cell Motil. *16*, 379–389.

Rayment, I., Holden, H.M., Whittaker, M., Yohn, C.B., Lorenz, M., Holmes, K.C., and Milligan, R.A. (1993). Structure of the actin-myosin complex and its implications for muscle contraction. Science *261*, 58–65.

Saez, C.G., Myers, J.C., Shows, T.B., and Leinwand, L.A. (1990). Human nonmuscle myosin heavy chain mRNA: generation of diversity through alternative polyadenylylation. Proc. Natl. Acad. Sci. USA *87*, 1164–1168.

Sanders, L.C., Matsumura, F., Bokoch, G.M., and de Lanerolle, P. (1999). Inhibition of myosin light chain kinase by p21-activated kinase. Science *283*, 2083–2085.

Satterwhite, L.L., Lohka, M.J., Wilson, K.L., Scherson, T.Y., Cisek, L.J., Corden, J.L., and Pollard, T.D. (1992). Phosphorylation of myosin-II regulatory light chain by cyclin-p34cdc2: a mechanism for the timing of cytokinesis. J. Cell Biol. *118*, 595–605.

Satterwhite, L.L., and Pollard, T.D. (1992). Cytokinesis. Curr. Opin. Cell Biol. *4*, 43–52.

Sellers, J.R. (1999). Myosins, 2nd ed., Oxford, UK: Oxford University Press.

Simons, M., Wang, M., McBride, O.W., Kawamoto, S., Yamakawa, K., Gdula, D., Adelstein, R.S., and Weir, L. (1991). Human nonmuscle myosin heavy chains are encoded by two genes located on different chromosomes. Circ. Res. *69*, 530–539.

Sohn, R.L., Vikstrom, K.L., Strauss, M., Cohen, C., Szent-Gyorgyi, A.G., and Leinwand, L.A. (1997). A 29 residue region of the sarcomeric myosin rod is necessary for filament formation. J. Mol. Biol. *266*, 317–330.

Toothaker, L.E., Gonzalez, D.A., Tung, N., Lemons, R.S., Le Beau, M.M., Arnaout, M.A., Clayton, L.K., and Tenen, D.G. (1991). Cellular myosin heavy chain in human leukocytes: isolation of 5′ cDNA clones, characterization of the protein, chromosomal localization, and upregulation during myeloid differentiation. Blood *78*, 1826–1833.

Tullio, A.N., Accili, D., Ferrans, V.J., Yu, Z.-X., Takeda, K., Grinberg, A., Westphal, H., Preston, Y.A., and Adelstein, R.S. (1997). Nonmuscle myosin II-B is required for normal development of the mouse heart. Proc. Natl. Acad. Sci. USA *94*, 12407–12412.

van Leeuwen, F.N., van Delft, V., Kain, H.E., van der Kammen, R.A., and Collard, J.G. (1999). Rac regulates phosphorylation of the myosin-II heavy chain, actinomyosin disassembly and cell spreading. Nat. Cell Biol. *1*, 242–248.

Verkhovsky, A.B., Svitkina, T.M., and Borisy, G.G. (1995). Myosin II filament assemblies in the active lamella of fibroblasts: their morphogenesis and role in the formation of actin filament bundles. J. Cell Biol. *131*, 989–1002.

Verkhovsky, A.B., Svitkina, T.M., and Borisy, G.G. (1997). Polarity sorting of actin filaments in cytochalasin-treated fibroblasts. J. Cell Sci. *110*, 1693–1704.

Warrick, H.M., and Spudich, J.A. (1987). Myosin structure and function in cell motility. Annu. Rev. Cell. Biol. *3*, 379–421.

Yamakita, Y., Yamashiro, S., and Matsumura, F. (1994). In vivo phosphorylation of regulatory light chain of myosin II during mitosis of cultured cells. J. Cell Biol. *124*, 129–137.

Zang, J.H., Cavet, G., Sabry, J.H., Wagner, P., Moores, S.L., and Spudich, J.A. (1997). On the role of myosin-II in cytokinesis: division of dictyostelium cells under adhesive and nonadhesive conditions. Mol. Biol. Cell *8*, 2617–2629.

Zang, J.H., and Spudich, J.A. (1998). Myosin II localization during cytokinesis occurs by a mechanism that does not require its motor domain. Proc. Natl. Acad. Sci. USA *95*, 13652–13657.